Journal of Food and Drug Analysis

Volume 31 | Issue 3 Article 8

Cordycepin inhibits ERK pathway to suppress FGF9-induced tumorigenesis with MA-10 mouse Leydig tumor cells

ORIGINAL ARTICLE

Cordycepin inhibits ERK pathway to suppress FGF9-induced tumorigenesis with MA-10 mouse Leydig tumor cells

Li-Ching Chen [a], Chin-Ying Chen [b], Yi-Ping Lee [b], Bu-Miin Huang [b,c,*]

[a] Department of Biological Science & Technology, China Medical University, Taichung, 406040, Taiwan, ROC
[b] Department of Cell Biology and Anatomy, College of Medicine, National Cheng Kung University, Tainan, 70101, Taiwan, ROC
[c] Department of Medical Research, China Medical University Hospital, China Medical University, Taichung, 40406, Taiwan, ROC

Abstract

Fibroblast growth factor 9 (FGF9) is a member of FGF family, and abnormal expression of FGF9 can promote tumorigenesis. Cordycepin, a major bioactive component in fungus *Cordyceps sinensis*, could suppress various tumors. We have shown that cordycepin could inhibit FGF9-induced testicular tumor growth *in vitro* and *in vivo* with MA-10 mouse Leydig tumor cells. In the present study, the mechanisms related to apoptosis and autophagy were determined. Results show that cordycepin significantly suppressed cell viability and colony formation with correlatedly morphological change related to cell death in FGF9-treated MA-10 cells. Flow cytometry and western blotting results further demonstrate that cordycepin induced apoptosis through the cleavage of caspase-8, -9, -3 and PARP in FGF9-treated MA-10 cells. However, the expressions of LC3-II, beclin-1 and p62 were not stimulated by cordycepin with the presence of FGF9, suggesting cordycepin would activate apoptosis, but not autophagy, in FGF9-treated MA-10 cells. Moreover, inhibition of ERK signal pathway and autophagy would enhance cordycepin-induced cell death effects in FGF9-treated MA-10 cells, referring that ERK signaling was regulated under cordycepin and FGF9 treatments. In NOD-SCID mouse allograft model inoculated with MA-10 cells, cordycepin significantly suppressed tumor growth with the presence of FGF9, and the cleavage of caspase-3 could be observed in tumor tissue, implying cordycepin induced caspase cascade to suppress tumor growth. Moreover, cordycepin plus U0126, ERK inhibitor, further significantly suppressed tumor growth with the presence of FGF9 as compared to the FGF9 only group, confirming the involvement of ERK signaling in this event. In conclusion, cordycepin induced caspase and ERK pathways to promote MA-10 cell apoptosis, but not autophagy, with the presence of FGF9.

Keywords: Apoptosis, Cordycepin, ERK Pathway, FGF9, MA-10 cells

1. Introduction

Fibroblast growth factor 9 (FGF9), a member of human FGF family, plays important roles including embryonic development [1], tissue repair [2], sex determination [3,4] and tumorigenesis [5]. Although FGF9 is indispensable to the human development, abnormal secretion of FGF9 has been reported to associate with several cancers, such as colorectal, endometrial and ovarian cancer [4]. In fact, irregular expression of FGF9 is closely associated with poor prognosis in patients with gastric cancer [6] and non-small cell lung cancer [7].

Cordycepin (3′-deoxyadenosine), an extract from the fungus *Cordyceps sinensis* of the traditional Chinese medicine, has been demonstrated with multiple physiological functions, such as anti-oxidative activity, immune system activation, anti-metastatic effects and anticancer action [8,9]. Studies have shown that cordycepin can induce anti-proliferation and apoptosis in liver cancer [10], lung cancer [11], and prostate cancer [12].

Mitogen-activated protein kinase (MAPK) cascades relate to many cellular regulations, including cell proliferation, differentiation, apoptosis, angiogenesis and tumor metastasis [13]. These cascades

Received 31 March 2023; accepted 17 May 2023.
Available online 31 August 2023

* Corresponding author at: Department of Cell Biology and Anatomy, College of Medicine, National Cheng Kung University, No. 1 University Road, Tainan, 70101, Taiwan, ROC. Fax: +886 6 209 3007.
E-mail address: bumiin@mail.ncku.edu.tw (B.-M. Huang).

https://doi.org/10.38212/2224-6614.3464

transmit signals through sequential activation of three to five layers of protein kinases, including extracellular signal-regulated kinase 1 and 2 (ERK1/2), c-Jun N-terminal kinase (JNK), and p38 mitogen-activated protein kinases (p38). Among them, ERK1/2 is one of the most dysregulated signaling pathway in human cancers [14]. Study has also shown that FGF/FGFR signaling pathway could induce MAPK pathway [15]. Because of this important role of MAPK pathway involved in cancer development, combination therapies with MAPK inhibitors become a biologically viable model for targeting cancer therapeutics [14].

Apoptosis, also called programmed cell death, is a process that is common to all multicellular organisms for eliminating cells via a complex but highly defined programmer [16]. Apoptotic cells are characterized by nuclear fragmentation, cell shrinkage and the formation of apoptotic bodies [17]. Apoptosis can be divided into two signaling pathways; the intrinsic pathway (mitochondrial pathway) and the extrinsic pathways (death receptor pathway). The extrinsic pathway is regulated by membrane death receptors, which are activated by binding between a ligand and its receptor [18]. The extrinsic pathway initiates through the ligation of cell-membrane death receptors to their corresponding natural ligands, which in turn stimulates the recruitment of the initiator caspase 8 [19,20]. The intrinsic pathway (mitochondrial pathway) is regulated by Bcl-2 protein family comprising of anti-apoptotic (like Bcl-2 and Bcl-XL) and pro-apoptotic (like Bax and Bak) factors, and its equilibrium determines outer mitochondrial membrane permeabilization [21], which leads to cytochrome-c release from mitochondrion inter-membrane space to the cytosol, stimulating caspase-9 activation and apoptosome formation [21–23]. Caspase-8 and caspase-9 can then directly cleave the downstream effector caspases-3/6/7 [24], resulting in poly ADP-ribose polymerase (PARP) cleavage to induce DNA fragmentation and apoptosis [20,23].

Autophagy is a catabolic process whereby cellular material is enclosed in the double-membrane autophagosomes and delivered to lysosomes for degradation [25]. Cells would replace old components with better-quality ones, and it requires synthesis of new components with the degradation of pre-existing materials, which can serve as building blocks [26]. When cells are under stress conditions, such as starvation, autophagy is initiated to protect cells. During periods of starvation, autophagy degrades cytoplasmic materials to produce amino acids and fatty acids that can be used to synthesize new proteins or are oxidized by mitochondria to produce ATP for cell survival [27].

Studies have identified autophagy-related (ATG) proteins could regulate autophagosome formation. However, it can result in autophagic cell death as autophagy is excessively induced [28,29]. There is cross-talk between autophagy and apoptosis, and the inhibition of autophagy may enhance apoptosis or autophagy could occur upstream of apoptosis [30]. It is illustrated when cells are under deprivation conditions of nutrients or growth factors, activation of 5′ adenosine monophosphate-activated protein kinase (AMPK) and/or inhibition of mammalian target of rapamycin (mTOR) could lead to activation of Unc-51 like kinase (ULK), which could phosphorylate beclin-1 to activate VPS34 with phagophore formation [31]. Multiple ATG proteins, such as ATG5 and ATG7, constitute two "ubiquitin–like conjugation systems" that catalyze the formation of phosphatidylethanolamine (PE)-conjugated LC3 (LC3-II) and direct its proper incorporation into the phagophore membrane [32]. The closure of an elongated phagophore marks the formation of a mature autophagosome, which eventually fuses with a lysosome, leading to cargo degradation and recycling of nutrients and metabolites [25]. In this process, p62/SQSTM1 and NIX help cells to identify and deliver misfolded or aggregated proteins and damaged organelles to the autophagosome for degradation [33].

Leydig cells residue in the interstitial region between seminiferous tubules in testis, and testosterone released from Leydig cells is regulated mainly by luteinizing hormone [34]. Testicular Leydig cell tumors are the most common non-germ cell gonadal tumors, although these tumors overall account for 1–3% of testicular tumors and usually occur in prepubertal boys (between 5 and 10 years) and men between 30 and 60 years [35].

Previously, we have shown that FGF9 could induce cell proliferation in MA-10 cells *in vitro* and *in vivo*, associated with testicular cancer developments [35]. We have also revealed the anticancer effect of cordycepin on FGF9-treated MA-10 cell tumor growth *in vitro* and *in vivo* through the regulation of p-ERK1/2, p-Rb, E2F1, cell cycle related proteins, and FGFR1-4 proteins [36]. However, whether cordycepin can induce apoptosis and/or autophagy in FGF9-induced testicular tumor remains elusive. Thus, in the present study, MA-10 mouse Leydig tumor cells were treated with cordycepin plus FGF9 *in vitro* and *in vivo*, and the mechanisms related to apoptosis and/or autophagy were investigated.

2. Materials and methods

2.1. Chemicals

Human Fibroblast Growth Factor 9 (FGF9) was purchased from PeproTech (Rocky Hill, NJ, USA). Ethanol was purchased from PerkinElmer (Boston, MA, USA). Bovine serum albumin (BSA), 30% acrylamide/Bis-acrylamide solution, methyl tetrazolium (MTT), dimethyl sulfoxide (DMSO), sodium chloride (NaCl), potassium chloride (KCI), 4-(2-hydroxyethyl)-1-piperazineethanesulfonic acid (HEPES), D-glucose and proteinase inhibitor, cordycepin, Waymouth MB 752/1 medium and sodium hydroxide (NaOH) were purchased from Sigma–Aldrich (St. Louis, MO, USA). Fetal bovine serum (FBS), Dulbecco's modified eagle medium nutrient mixture F-12 (D-MEM/F12) and trypsin–EDTA were purchased from Gibco (Grand Island, NY, USA). Sodium chloride (NaCl), Tris base and potassium chloride (KCI) were purchased from JT Baker (Phillipsburg, NJ, USA). Hydrochloric acid (HCl), acetic acid and sodium dodecyl sulfate (SDS) were purchased from Merck (Darmstadt, Germany). Tween-20 was purchased from AppliChem (Darmstadt Germany). Peroxidase AffiniPure goat anti-rabbit IgG (H + L) was purchased Jackson ImmunoResearch Inc. (West Grove, PA, USA) and donkey anti-mouse IgG conjugated with horseradish peroxidase was purchased from PerkinElmer (Boston, MA, USA). Monoclonal antibodies against phosphor-ERK1/2 (1:4000; #9101), ERK1/2 (1:4000; #9102), cleaved caspase-3 (1:2000; #9661) and Atg12 (1:2000; #4180); and polyclonal antibodies against cleaved caspase-8 (1:1000; # 9429), cleaved caspase-9 (1:1000; #9509), PARP (1:1000; #9542), LC3A/B (1:1000; #4108), and Beclin-1 (1:1000; #3738) were purchased from Cell Signaling (Beverly, MA, USA). Polyclonal antibody against SQSTM1/P62 (1:3000; #GTX100685) was purchased from GeneTex (Irvine, CA, USA). Polyclonal antibodies against Bcl-2 (1:1000; #12789-1-AP) and β-actin (1:8000; #20536-1-AP) were purchased from Proteintech (Rosemont, CA, USA). Enhanced chemiluminescence (ECL) detection kit was purchased from Millipore (Billerica, MA, USA). Annexin V-FITC apoptosis detection kit was purchased from Strong Biotech (Taipei, TAIWAN).

2.2. Cell culture

MA-10 cell line was a gift from Dr. Mario Ascoli (University of Iowa, Iowa City, IA, USA) and cultured in the Waymouth MB 752/1 medium with 10% FBS. All the cells were maintained in a humidified incubator at 37 °C with 5% CO_2.

2.3. MTT viability test

MA-10 cells were seeded 8×10^3 cells in 96-well plates per well with 200 μL culture medium. After incubation for 20–24 h for seeding, cells were changed to serum free medium for 18 h. After starvation, cells treated with BSA (vehicle control), 50 ng/mL FGF9, DMSO (vehicle control) and/or different concentrations of cordycepin (20, 5, 50 or 100 μM) in medium containing 1% FBS for 12 and 24 h, respectively. Then, MTT was added to each well (0.5 mg/mL final concentration) and incubated in humidified incubator at 37 °C with 5% CO_2 for 3 h. After discarding the medium, 50 μL DMSO was added into each well and placed on the shaker to dissolve the crystals for 30 min in dark. The cell viability was then detected at $\lambda = 570$ nm by VersaMax ELISA reader (Molecular Devices, Sunnyvale, CA, USA).

2.4. PrestoBlue™ cell viability assay

MA-10 cells were seeded 8×10^3 cells in 96-well plates per well with 200 μL culture medium. After treatments, medium was removed and 10 μL PrestoBlue Reagent was added with 90 μL 1% FBS medium directly to cells, and then incubation for 1.5 h at 37 °C in dark. The cell viability was detected at $\lambda = 570$ nm and, using 600 nm as a reference wavelength (normalized to the 600-nm value) by VersaMax ELISA reader (Molecular Devices, Sunnyvale, CA, USA). Cell viabilities were calculated according to PrestoBlue™ Cell Viability Reagent protocol (Thermo Fisher, Waltham, MA, USA).

2.5. Morphology observation

MA-10 cells were seeded at a concentration of 5.5×10^5/mL for 12 h and 4×10^5/mL for 24 h in 6-cm culture dishes with 2 mL culture medium. After incubating for 20–24 h for seeding, cells were changed to serum free medium for 18 h. After starvation, cells were treated with BSA (vehicle control), 50 ng/mL FGF9, DMSO (vehicle control) and/or different concentrations of cordycepin (0, 25, 50 or 100 μM) in MA-10 cells for 12 and 24 h, respectively. Cell morphology was then observed under Olympus CK40 light microscopy, and the images were recorded by Olympus DP20 digital camera (Olympus, Tokyo, Japan).

2.6. Clonogenic assay

Cells were treated with BSA (vehicle control) or 50 ng/mL FGF9, and cordycepin was then added to

the cells at different concentrations (0, 25, 50 or 100 μM) or DMSO (vehicle control). Then, cells were trypsinized and subsequently replated with 1000–1500 cells in 6-cm culture dishes and returned to the incubator to allow for colony development. After 8–14 days, colonies (containing ≥50 cells in each colony) were stained with 0.5% crystal violet solution. Results in line graphs are mean ± standard error with at least 3 independent experiments. The plating efficiency (PE) is the ratio of the number of colonies to the number of cells seeded in culture dishes. The surviving fraction (SF) was calculated as follows: SF = plating efficiency (PE) of treated cells/PE of control cells. PE (%) was obtained from (colonies counted/cell plated) × 100. Survival curves were then plotted using the mean surviving fraction values [37].

2.7. Protein collection and western blotting

MA-10 cells were seeded at a concentration of 5.5×10^5 cells for 12 h and 4×10^5 cells for 24 h, respectively, in 6-cm culture dishes with 2 mL culture medium. After treatment, cells were washed with cold PBS twice and cell suspensions were centrifuged at 1000 rpm for 3 min at 25 °C. Attached cells were lysed with 50–70 μL lysis buffer (20 mM Tris pH 7.5, 150 mM NaCl, 1 mM EDTA, 1 mM EGTA, 1% Triton X-100, 2.5 mM sodium pyrophosphate, 1 mM β-Glycerolphosphate and 1 mM Na_3VO_3) with proteinase inhibitor and centrifuged at 12000×*g* for 12 min at 4 °C. Cell suspensions were collected and stored at −80 °C. Protein concentrations of cell lysates were determined by Bio-Rad protein assay dye reagent concentrate (Bio-Rad Laboratories, Hercules, CA, USA). For Western blotting, cell lysates containing 25–35 μg protein were resolved in 12% SDS-PAGE gel with standard running buffer (24 mM Tis-HCl, 0.19 M glycine, and 0.5% sodium dodecyl sulfate, pH 8.3) at room temperature, and electrophoretically transferred onto polyvinylidene difluoride (PVDF) membrane on ice. Electrophoresis was performed at 90 V and transferred onto PVDF membrane was performed at 375 mA for 90 min. PVDF membrane with transferred protein was incubated in blocking buffer (5% non-fat milk in 0.1% TBST washing buffer) for 1 h and incubated with primary antibodies for 16–18 h at 4 °C. Membranes were washed 3 times with TBST and incubated with the appropriate dilution of HRP-conjugated secondary antibodies for 1 h. Signaling was visualized through UVP EC3 BioImaging Systems (UVP, Upland, CA, USA) by ECL detection kit [38]. The quantificational analysis was analyzed with ImageJ program version 1.5 (NIH, Bethesda, MD, USA).

2.8. Annexin V/PI double staining assay

After harvesting by trypsin and washing by 2 mL culture medium, cell suspensions were centrifuged at 1000 rpm for 3 min at 4 °C. The pellets were washed twice with cold PBS and centrifuged again. Cellular apoptosis was detected by FITC Annexin V Apoptosis Detection Kit according to manufacturer's standard protocol (BD Pharmingen™, Franklin Lakes, NJ, USA). Cells were resuspended in 100 μL 1X binding buffer at a concentration of 1×10^6 cells/mL to 1.5 mL eppendorf. Then, 5 μL of FITC Annexin V and 5 μL PI were added to the cells in eppendorf solution and vortexed. After incubated at room temperature in the dark for 15 min, 400 μL of 1X binding buffer was added to each tube, and then analyzed by CytoFLEX flow cytometer (Beckman Coulter, Brea, CA, USA).

2.9. Signal pathway confirmation with inhibitors

MA-10 cells were pre-treated with MAPK inhibitor (U0126), caspase pan inhibitor (Z-VAD-FMK) or autophagy inhibitor chloroquine (CQ) for 1 h, and then treated with/without FGF9 and different concentrations of cordycepin (0 and 50 μM). Prestoblue assay and annexin V/PI double staining assay were further exploited to confirm what pathway(s) was/were activated by cordycepin in FGF9-treated MA-10 cells, respectively.

2.10. Animals and allograft tumor analysis

Five weeks old male NOD-SCID mice were purchased from National Cheng Kung University Animal Center (Tainan, Taiwan). Experimental procedures were consistent with ethical principles for animal research which were approved by the Institutional Animal Care and Use Committee of National Cheng Kung University. Environmental conditions for mouse were kept at temperature of 22°C–24 °C and a constant 12-h light/dark cycle.

Mice were subcutaneously injected in the back region with 1×10^6 MA-10 cells suspended in 0.1 mL Waymouth medium. Tumors were allowed to grow for 7–12 days and mice were randomly assigned to 5 groups: (A) intratumor injection of 0.1% BSA together with intraperitoneal of DMSO; (B) intratumor injection of 50 ng/mL FGF9 together with intraperitoneal of DMSO; (C) intratumor injection of 50 ng/mL FGF9 together with intraperitoneal of cordycepin (20 mg/kg) and U0126 (10.5 mg/kg); (D) intratumor injection of 0.1% BSA together with intraperitoneal of cordycepin (20 mg/kg); and (E) intratumor injection of 50 ng/mL FGF9 together with intraperitoneal of cordycepin (20 mg/kg). Injection of

FGF9, cordycepin and/or U0126 was given daily for first week and then injected every other day for 6 more days. The size of tumor was measured with a clipper every other day, and the tumor volume was calculated using formula V= (L × W × W × 0.52) [39]. Mice were sacrificed on the 13th day after drug administration, and tumors were collected for specific protein detections by immunohistochemistry staining.

2.11. Immunohistochemistry staining

MA-10 tumor tissues were soaked in a 10% neutral buffered formalin (BIOTnA Biotech, Kaohsiung, TAIWAN) over 3 days. The paraffin sections were dewaxed in xylene, dehydrated in ethanol, and washed in PBS. Sodium citrate buffer (pH 6.0) was used to retrieve the antigen for 50 min at 120 °C autoclave. Endogenous peroxidase activity was

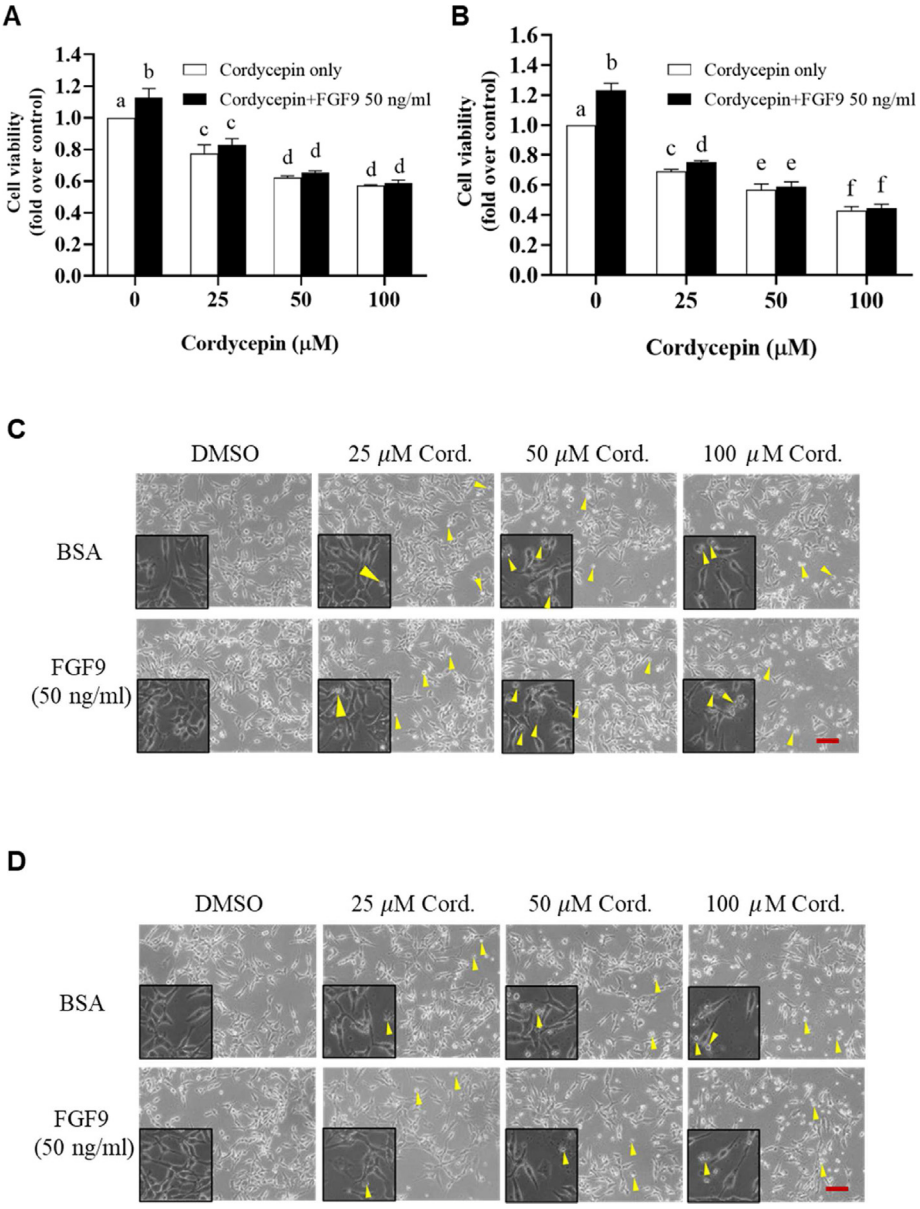

Fig. 1. ***Cordycepin suppresses FGF9-treated MA-10 cell proliferation.*** *After 18 h serum starvation, MA-10 cells were co-treated without or with 50 ng/mL FGF9 and 0, 25, 50 and 100 μM cordycepin for 12 (A) and 24 h (B) with 1% bovine serum albumin (BSA), respectively. Microscopic examination of morphological changes was observed under light microscopy in 6 cm dish, and cells were co-treated without or with 50 ng/mL FGF9 and 0, 25, 50 and 100 μM cordycepin for 12 (C) and 24 h (D), respectively. Results are mean ± standard error with at least 3 independent experiments. One-way ANOVA with Tukey's multiple comparisons post-tests in (A) and (B) were used to determine the statistical difference. Different alphabetical letters above bars represent statistical differences among different treatments; $p < 0.05$. Yellow arrowhead indicates cell membrane blebbing in (C) and (D) (red scale bar, 50 μm), and the inset is x4 enlarged image of cell membrane blebbing from each corresponding figure (DMSO = Dimethyl sulfoxide; Cord. = cordycepin).*

blocked by incubation with 0.3% H_2O_2 followed with PBS. The paraffin sections were blocked with 2% milk and 2 μL/mL goat IgG in blocking buffer for 1 h. The primary antibody cleaved caspase-3 (1:200), CD-31 (1:200) and phosphor-ERK (1:100) incubated in 4 °C refrigerator overnight. Next day, sections were washed with PBS, Diaminobenzidine (DAB) buffer was used to reveal the desired signals and hematoxylin was used to stain cell nuclear. After washing, all sections were dehydrated by graded ethanol series, cleared in xylene, and covered with a coverslip in mounting gel (Merck, Darmstadt, Germany). Immunohistological sections were examined with a light microscope (Zeiss, AX10, Thornwood, NY). DAB positive area was analyzed with the "area detection" measurement method with ImageJ program version 1.5 (NIH, Bethesda, MD, USA).

2.12. Statistical analysis

The data are expressed as mean ± SEM of at least three separate experiments. Statistical significance of differences between control and treatment groups was determined by two-way ANOVA followed by Tukey multiple comparisons test, using GraphPad Prism 8 (GraphPad Software, San Diego, CA, USA), and statistical significance was set at $p < 0.05$.

3. Results

3.1. Cordycepin decreased FGF9-induced MA-10 cell viability

We have shown cordycepin could suppress FGF9-induced MA-10 cell tumorigenesis *in vitro* and *in vivo* [35]. To confirm the phenomena in the present study, MA-10 cells were treated without or with FGF9 plus cordycepin (0, 25, 50 and 100 μM) for 12 and 24 h, respectively, and cell viabilities were determined by MTT assay. Results showed again that cordycepin alone (25, 50 and 100 μM) significantly suppressed MA-10 cell viability at 12 (Fig. 1A) and 24 h (Fig. 1B) in dose-dependent manners, respectively. The 50 ng/mL FGF9 alone did increase cell viability at 12 (Fig. 1A) and 24 h (Fig. 1B). However, cordycepin (25, 50 and 100 μM) could also still significantly

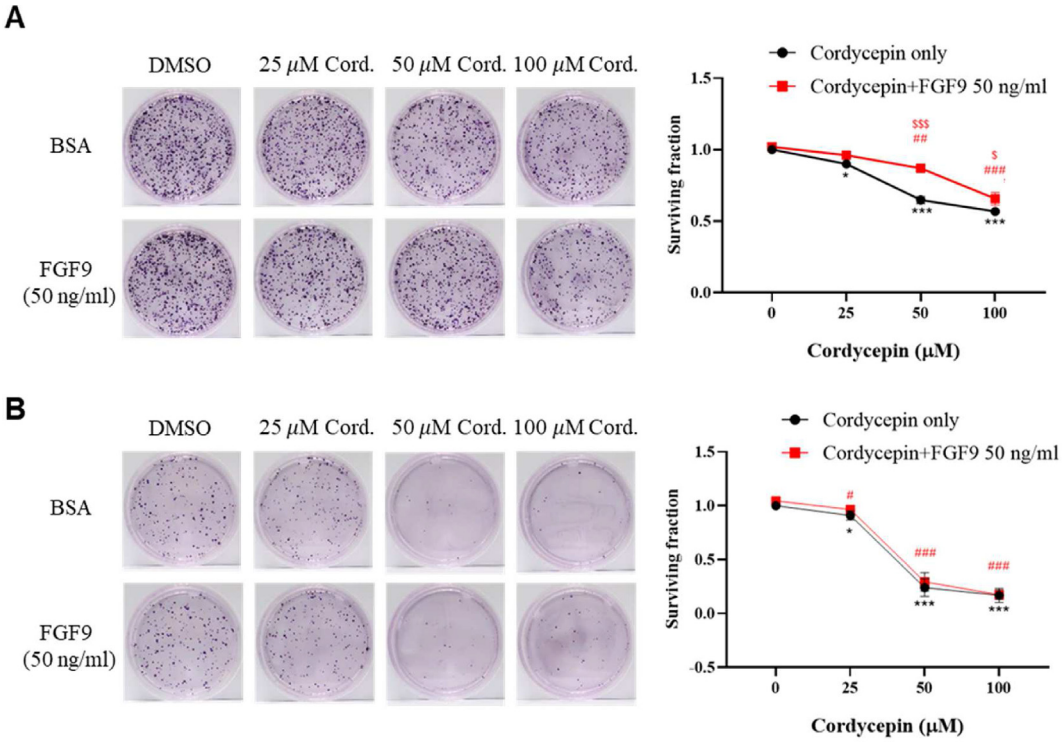

Fig. 2. ***Cordycepin decreases FGF9-treated MA-10 cell colony formation.*** *The 1500 MA-10 cells were co-treated without or with 50 ng/mL FGF9 and 0, 25, 50 and 100 μM cordycepin in 6-cm culture dishes for 12 (A) and 24 (B) h, respectively. Number of colony formation between different treatments were then counted, which were further analyzed by two-way ANOVA with Tukey's multiple comparisons post-tests. The *$p < 0.05$ and ***$p < 0.001$ represent significant difference between control and cordycepin only (25, 50 and 100 μM) treatments. The $^{\#}p < 0.05$, $^{\#\#}p < 0.01$ and $^{\#\#\#}p < 0.001$ represent significant difference between FGF9 alone and FGF9 plus cordycepin (25, 50 and 100 μM) treatments. The $^{\$}p < 0.05$ and $^{\$\$\$}p < 0.001$ represent significant difference between cordycepin only (50 and 100 μM) and FGF9 plus cordycepin (50 and 100 μM) treatments (DMSO = Dimethyl sulfoxide; Cord. = cordycepin).*

suppress MA-10 cell viability at 12 (Fig. 1A) and 24 h (Fig. 1B), respectively, with the presence of 50 ng/mL FGF9 in dose-dependent manners.

Upon cell morphological changes, most MA-10 cells illustrated spindle shapes in control group, but cell number with rounded-up, or even shrunk/condensed, phenomena increased under 50 and 100 μM cordycepin alone at 12 and 24 h treatments, respectively (Fig. 1C and D). Remarkably, number of the rounded-up MA-10 cells decreased in 50 and 100 μM cordycepin with the presence of 50 ng/mL FGF9 treatment as compared to cordycepin alone treatment, especially at 24 h (Fig. 1C and D).

3.2. Cordycepin decreased FGF9-induced MA-10 cell colony-forming ability

Colony formation assay is a method to define the ability of a single cell to grow into a colony, illustrating cell viability [37]. After treatments without or with 50 ng/mL FGF9 plus different concentration of cordycepin (0, 25, 50 and 100 μM) for 12 and 24 h, respectively, MA-10 cells were incubated for extra 8–14 days to allow the formation of cell colonies. Results showed that cordycepin alone at 25, 50 and 100 μM did significantly suppress MA-10 cell colony-forming at 12 and 24 h treatments in a dose-dependent manner. With the presence of 50 ng/mL FGF9, colony formation was still significantly inhibited by 50 and 100 μM cordycepin at 12 h (Fig. 2A) and by 25, 50 and 100 μM cordycepin at 24 h (Fig. 2B), respectively. However, with the presence of 50 ng/mL FGF9, the suppressive effect of cordycepin at 50 and 100 μM was less at 12 h treatment as compared to 24 h treatment (Fig. 2A and B). It should be noted that colony numbers between FGF9 alone and BSA control groups didn't show statistical difference. However, FGF9 alone group approximately have darker staining upon cell colonies, illustrating cell number seemed to be higher in FGF9 alone group as compared to control group. These results illustrate that cordycepin could significantly decrease colony-forming in FGF9-treated MA-10 cells.

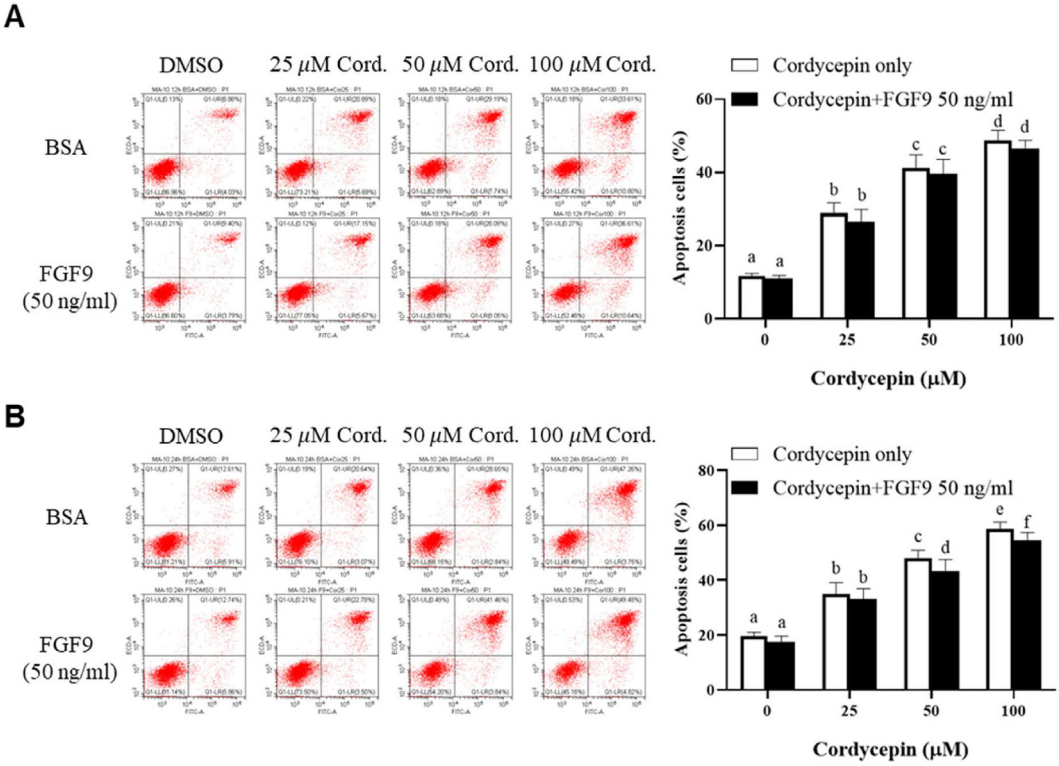

Fig. 3. ***Cordycepin-induced MA-10 cell apoptosis in the presence or absence of FGF9.*** *After cotreatment without or with 50 ng/mL FGF9 and 0, 25, 50, and 100 μM cordycepin for 12 (**A**) and 24 h (**B**), respectively, MA-10 cells were stained with annexin V and propidium iodide (PI), and then analyzed by flow cytometry to determine cell apoptotic status. Percentages of double-positive (late apoptotic), annexin V single-positive (early apoptotic), PI single-positive (necrotic) and double-negative (viable) cells are illustrated. Results in bar graphs are mean ± standard error with at least 3 independent experiments. Percentages of double-positive (late apoptotic) plus annexin V single-positive (early apoptotic) cells between treatments were then analyzed by two-way ANOVA with Tukey's multiple comparisons post-tests. Different alphabetical letters above bars represent statistical differences among different treatments; $p < 0.05$ (DMSO = Dimethyl sulfoxide; Cord. = cordycepin).*

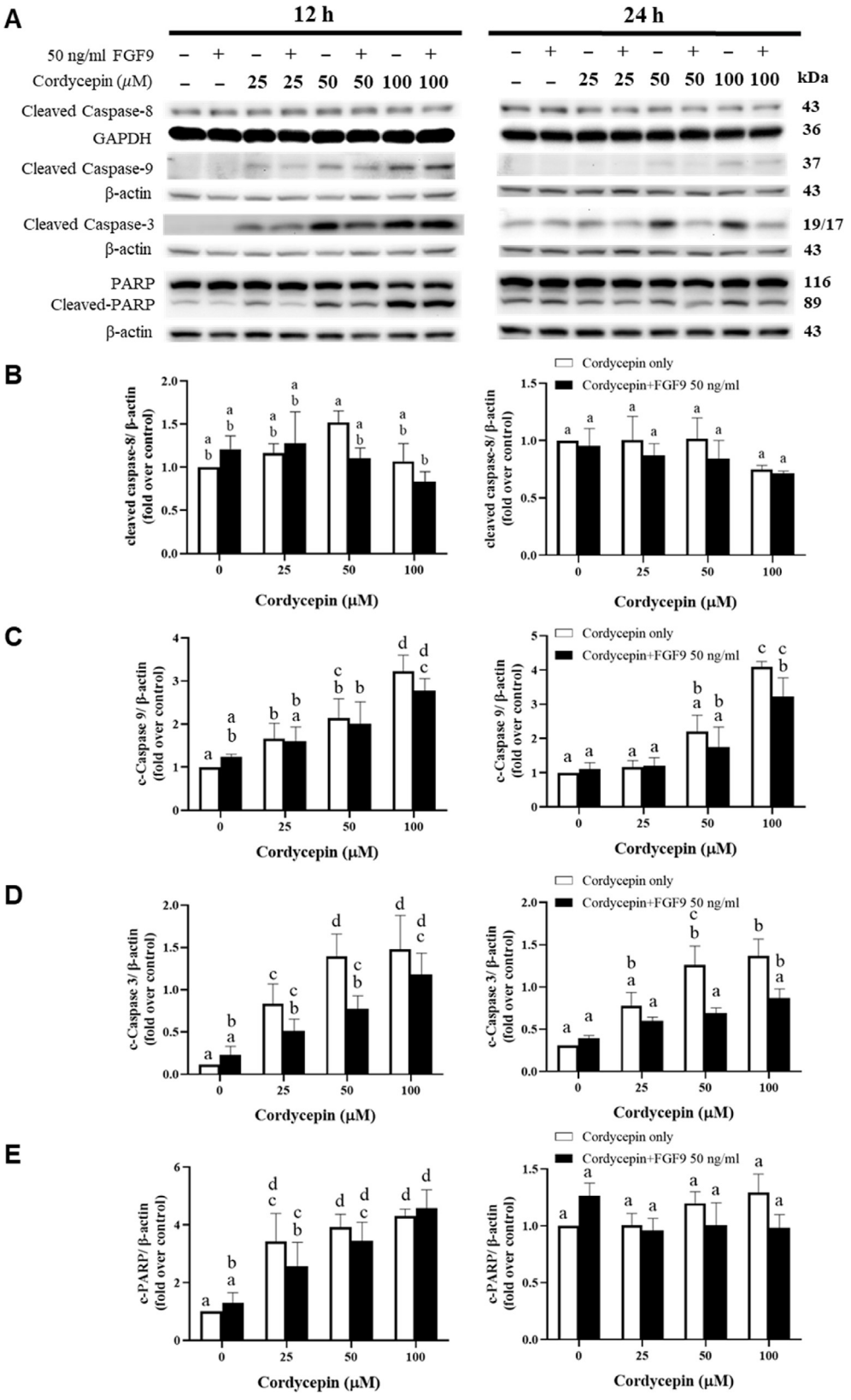

Fig. 4. ***Cordycepin induces apoptosis related protein expressions in FGF9-treated MA-10 cells.*** *MA-10 cells were co-treated without or with 50 ng/mL FGF9 and 0, 25, 50 and 100 μM cordycepin for 12 and 24 h, respectively. Western blot analysis for the expressions of cleaved caspase-8 (43 kDa) (**A** and **B**), cleaved caspase-9 (37 kDa) (**A** and **C**), cleaved caspase-3 (19/17 kDa) (**A** and **D**), and cleaved PARP (89 kDa) (**A** and **E**) in MA-*

10 cells were examined. Results in bar graphs are mean ± standard error with at least 3 independent experiments. Two-way ANOVA with Tukey's multiple comparisons post-tests were used to determine differences among different treatments. Different alphabetical letters above bars represent statistical differences among different treatments; $p < 0.05$.

3.3. Cordycepin induced FGF9-treated MA-10 cell apoptosis

To investigate the cell death mechanism, MA-10 cells were treated without or with 50 ng/mL FGF9 plus different concentration of cordycepin (0, 25, 50 and 100 μM) for 12 and 24 h, respectively, and cell apoptotic phenomena were detected by annexin V/PI double staining assay using flow cytometry. Results show that cordycepin alone at 25, 50 and 100 μM significantly induced MA-10 cell apoptosis at 12 and 24 h treatments, respectively (Fig. 3A and B). However, 50 ng/mL FGF9 did significantly reduce MA-10 cell apoptotic phenomena induced by 50 and 100 μM cordycepin, especially at 24 h treatment (Fig. 3B). These results demonstrate that cordycepin could significantly induce MA-10 cell apoptosis in FGF9-treated MA-10 cells.

3.4. Cordycepin induced cell death through caspase cascade in FGF9-treated MA-10 cells

The caspase cascade plays vital role in the induction, transduction and amplification of intracellular apoptotic signals [40]. Our laboratory previously showed that cordycepin could induce MA-10 cell apoptosis [35,41]. We have also observed that cordycepin inhibited FGF9-induced testicular tumor growth by affecting the expressions of p-ERK1/2, p-Rb, E2F1, and cell cycle related proteins [35]. In this study, how cordycepin interacted with FGF9 inducing caspase cascade in MA-10 cells were examined by western blotting assay.

Results show that cleaved caspase-8 was not induced by cordycepin without or with the presence of FGF9 in MA-10 cells at 12 and 24 h treatments (Fig. 4A and B). However, cordycepin at 25, 50 and 100 μM did significantly increase cleaved caspase-9 expression in a dose-dependent relationship at 12 h treatment, while cordycepin only at 100 μM significantly increased cleaved caspase-9 expression at 24 h treatment (Fig. 4A and C). With the presence of 50 ng/mL FGF9, only 100 μM cordycepin significantly increased cleaved caspase-9 expression at 12 and 24 h treatment (Fig. 4A and C).

Cordycepin at 25, 50 and 100 μM also significantly increased cleaved caspase-3 expression in a dose-dependent relationship at 12 and 24 h treatments, respectively (Fig. 4A and D). With the presence of FGF9, cordycepin at 100 μM also significantly increased cleaved caspase-3 expression at 12 h treatment. Although there was no significant difference of cleaved caspase-3 expression at 24 h treatment of cordycepin with the presence of FGF9, there was an increasing trend of cleaved caspase-3 expression (Fig. 4A and D).

Interestingly, FGF9 would significantly reduce the stimulatory effects of 50 μM cordycepin on cleaved caspase-3 expression at 12 and 24 h treatments, respectively, as compared with the same dose of cordycepin only group, illustrating FGF9 on cell proliferative effect could counteract the apoptotic effect of cordycepin in MA-10 cells. But, cordycepin could still significantly induce MA-10 cell apoptosis with the presence of FGF9 (Fig. 4A and D).

Cleaved PARP expression could be significantly induced by cordycepin at 25, 50 and 100 μM) at 12 h treatment, but not at 24 h (Fig. 4A and E). With the presence of FGF9, cordycepin at 25, 50 and 100 μM also significantly increased cleaved PARP expression at 12 h treatment, but not at 24 h (Fig. 4A and E). These results show that cordycepin could significantly activate caspase pathway to induce MA-10 cell apoptosis without or with the presence of FGF9.

3.5. Cordycepin didn't induce apoptosis through autophagy regulation in FGF9-treated MA-10 cells

To know whether cordycepin could also induce MA-10 cell autophagy for apoptosis, the expression of autophagy-related proteins, such as LC3 II, Atg5-12, beclin-1 and p62, in MA-10 cells with FGF9 (0 and 50 ng/mL) and/or cordycepin (0, 25, 50 and 100 μM) for 12 and 24 h treatments were investigated, respectively, by western blotting assay. Results show that FGF9 and/or cordycepin didn't have any effect on LC3 II/I ratio at 12 and 24 h treatments (Fig. 5A and B).

Crodycepin alone didn't have any effect on Atg5-12 expression at 12 h treatment, but did suppress it at 24 h treatment (Fig. 5A and C). With the presence of FGF9, cordycepin at 100 μM significantly suppressed Atg5-12 expression at 12 and 24 h treatments (Fig. 5A and C).

FGF9 and/or cordycepin didn't have any effect on beclin-1 ratio at 12 and 24 h treatments (Fig. 5A and D).

Crodycepin alone didn't have any effect on p62 expression at 12 and 24 h treatment (Fig. 5A and E). With the presence of FGF9, cordycepin at 100 μM significantly suppressed p62 expression at 12 h treatment, but not at 24 h treatment (Fig. 5A and E).

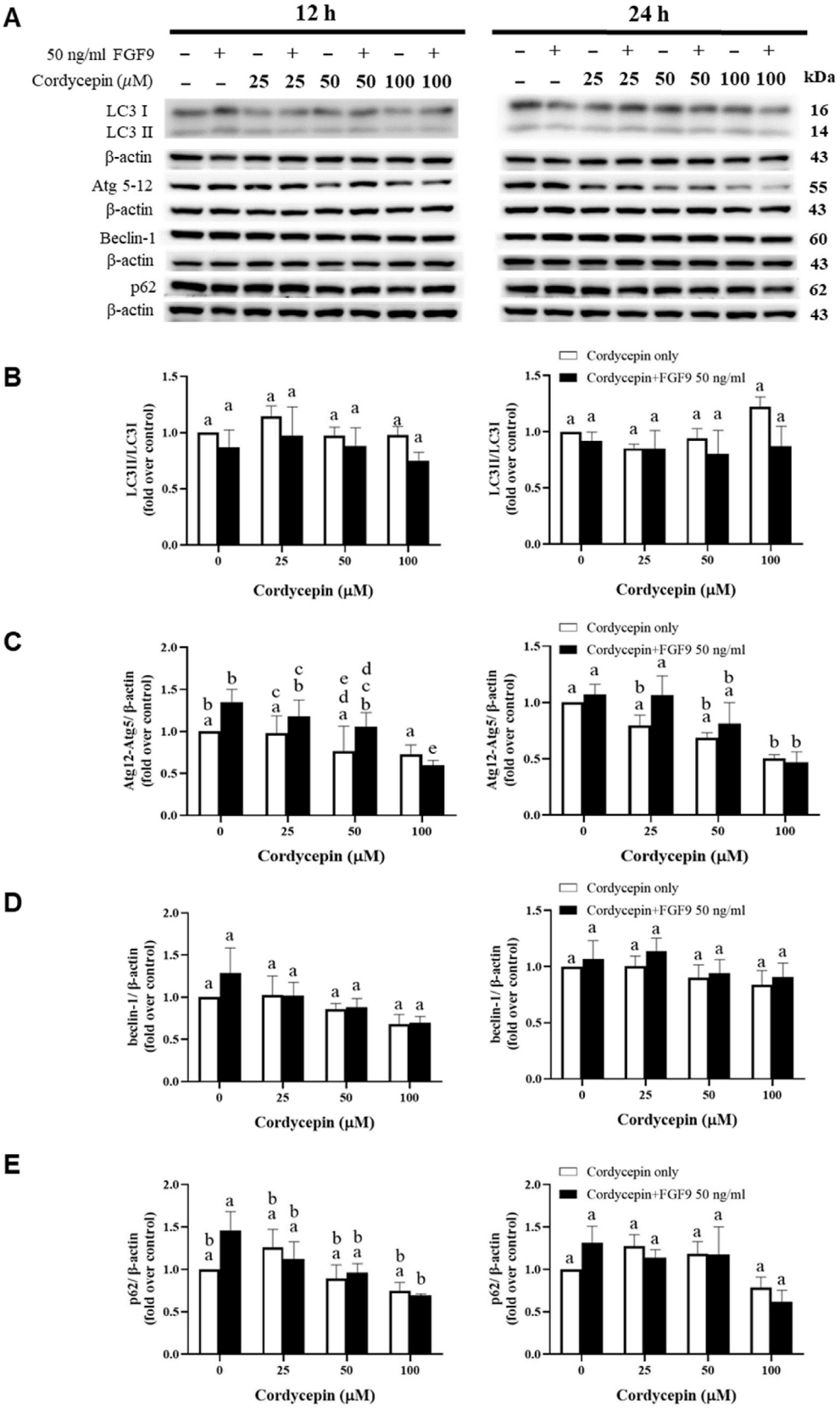

Fig. 5. ***Cordycepin induces expression of autophagy-related proteins in FGF9-treated MA-10 cells.*** *MA-10 cells were co-treated without or with 50 ng/mL FGF9 and 0, 25, 50 and 100 μM cordycepin for 12 and 24 h, respectively. Western blot analysis for the expressions of LC3 I/II (**A** and **B**), Atg5-12 (**A** and **C**), beclin-1 (**A** and **D**) and p62 (**A** and **E**) in MA-10 cells were examined. Results in bar graphs are mean ± standard error with at least 3 independent experiments. Two-way ANOVA with Tukey's multiple comparisons post-tests were used to determine differences among different treatments. Different alphabetical letters above bars represent statistical differences among different treatments; $p < 0.05$.*

These data suggest that cordycepin didn't regulate autophagy upon FGF9-induced MA-10 cell apoptosis.

3.6. Autophagy inhibition enhanced cordycepin-induced cell death effect in FGF9-treated MA-10 cells

There are many cross-talks between autophagy and apoptosis, in which the inhibition of autophagy may enhance apoptosis as autophagy occurs upstream of apoptosis [30]. In the present experiment, chloroquine (CQ), a classic inhibitor of autophagy that blocks the binding of autophagosomes to lysosomes [42], was used to treat MA-10 cell for blocking autophagy, and the cell viability under cordycepin and/or FGF9 treatments was detected by PrestoBlue assay.

MA-10 cells were pre-treated with CQ (50 uM) for 1 h, and then FGF9 (50 ng/mL) and/or cordycepin (0 and 50 μM) for 24 h. Data show that FGF9 could stimulate MA-10 cell viability, and cordycepin could reduce it without or with the presence of FGF9. Interestingly, CQ plus cordycepin could suppress more FGF9-induced MA-10 cell viability (Fig. 6A). These results indicate that inhibition of autophagy would enhance cordycepin-induced cell death effects in FGF9-treated MA-10 cells.

3.7. MEK inhibition enhanced cordycepin-induced cell death effect in FGF9-treated MA-10 cells

We have shown that FGF9 would induce ERK signal pathway to increase cell proliferation in MA-10 cells, and cordycepin could inhibit ERK signal pathway to reduce MA-10 cell growth [35,41]. To confirm that FGF9 and/or cordycepin could regulate ERK signaling pathway, MA-10 cell viability with the treatment of U0126 (ERK specific inhibitor) was detected by PrestoBlue assay. Results show that FGF9 could significantly induce the cell viability, and cordycepin inhibited FGF9-induced MA-10 cell viability (Fig. 6B). Interestingly, U0126 could augment cordycepin to decrease more FGF9-induced MA-10 cell viability (Fig. 6B), indicating that inhibition of ERK signal pathway would enhance cordycepin-induced cell death effects in FGF9-treated MA-10 cells.

Then, annexin V/PI double staining assay and flow cytometry were used to confirm whether FGF9 and/or cordycepin could regulate ERK and/or caspase pathways to induce MA-10 cell apoptosis. Results show that FGF9 at 50 ng/mL didn't induce any MA-10 cell apoptosis as compared to control (Fig. 6C). Cordycepin (50 μM) for 24 h significantly induced MA-10 cell apoptosis (Fig. 6C). Cordycepin (50 μM) for 24 h also significantly induced MA-10 cell apoptosis with the presence of FGF9 (50 ng/mL) (Fig. 6C). Interestingly, U0126 could induce further more apoptotic cells with the presence of cordycepin plus FGF9 as compared to cordycepin only or cordycepin plus FGF9 groups (Fig. 6C). Indeed, U0126 alone or U0126 plus FGF9 would also induce MA-10 cell apoptosis as compared to control or FGF9 alone groups (Fig. 6C). Fascinatingly, U0126 plus cordycepin could induce much more MA-10 cell apoptosis as compared to cordycepin alone, cordycepin plus FGF9, cordycepin plus FGF9 and U0126 groups (Fig. 6C).

In apoptotic event, Z-VAD-FMK alone (pan-caspase inhibitor) and Z-VAD-FMK plus FGF9 didn't have any effect on MA-10 cell apoptosis (Fig. 6C). However, Z-VAD-FMK did significantly decrease MA-10 apoptotic cell numbers in cordycepin only and cordycepin plus FGF9 groups, respectively (Fig. 6C).

These data suggest that cordycepin induced FGF9-treated MA-10 cell apoptosis through caspase and ERK pathways, and the suppression of ERK signaling pathway could enhance the apoptotic effect in MA-10 cells.

3.8. Cordycepin suppressed FGF9-induced MA-10 cell tumorigenesis in NOD-SCID allograph mouse model

Above results demonstrate that cordycepin could decrease FGF9-promoted MA-10 cell proliferation *in vitro* through caspase and/or ERK signaling pathways. Thus, NOD-SCID allograph mouse model was used to further determine whether cordycepin could have an inhibitory effect on FGF9-induced MA-10 cell tumorigenesis *in vivo*. In addition, ERK inhibitor (U0126) was also applied in this *in vivo* study to again confirm the role of ERK signaling pathway in FGF9-induced MA-10 cell tumorigenesis.

Results show that 50 ng/mL FGF9 significantly increased tumor volume from 9th to 13th day as compared to BSA control group, illustrating FGF9 only could significantly promote MA-10 cell tumorigenesis *in vivo* (Fig. 7A). Cordycepin only did significantly suppress tumor volume growth without FGF9 presence from 3rd to 13th day (Fig. 7A). Most importantly, cordycepin could significantly suppress tumor growth with the presence of FGF9 from 3rd to 13th day (Fig. 7A). Furthermore, cotreatment of cordycepin and U0126 also significantly suppressed tumor growth with the presence of FGF9 from 3rd to 13th day as compared to the FGF9 only group (Fig. 7A).

Regarding tumor size, mice in cordycepin only group had smallest size and mice in FGF9 only

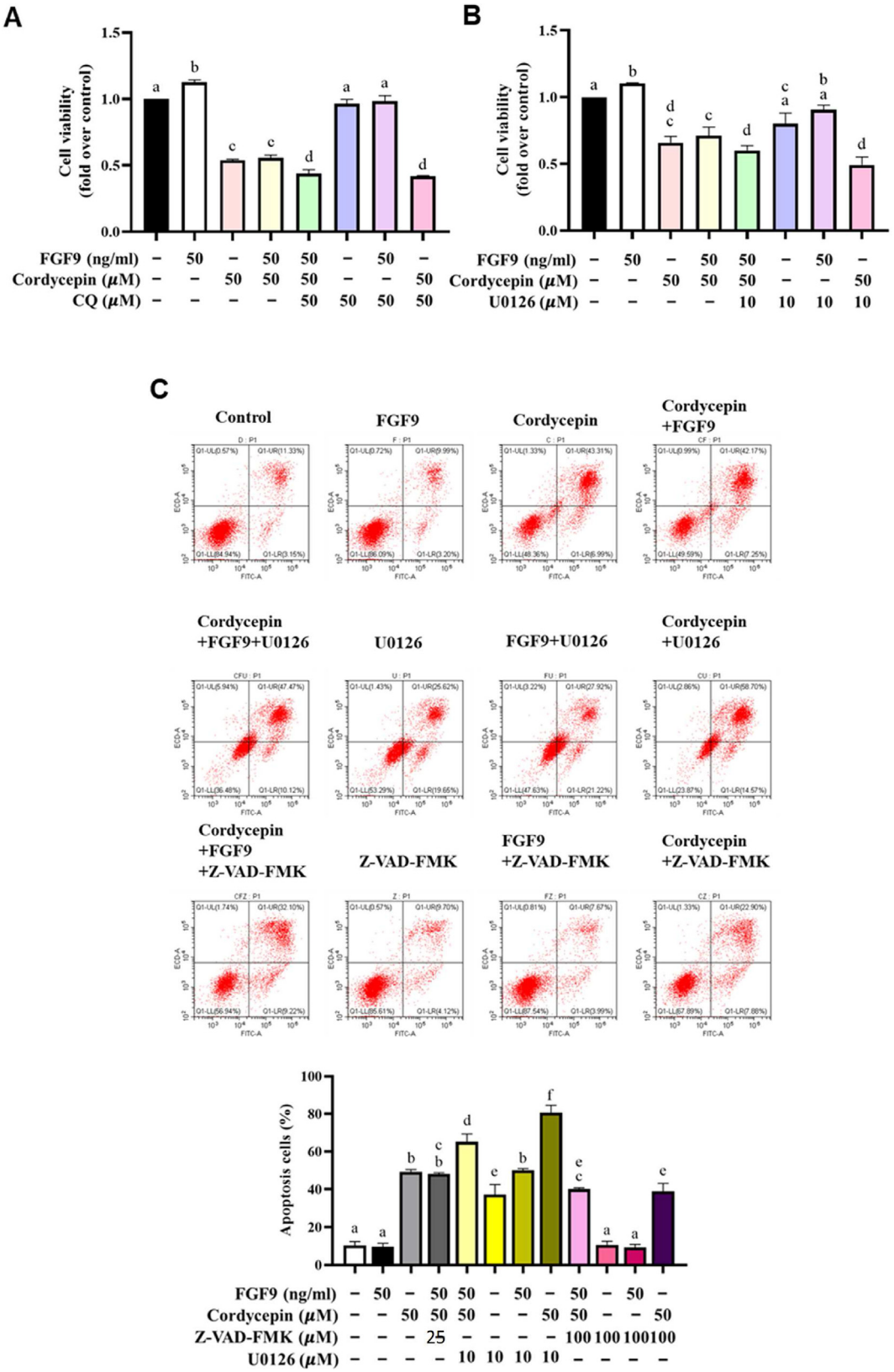

Fig. 6. ***Cordycepin induced antiproliferative effects through autophagy, ERK and caspase pathways in FGF9-treated MA-10 cells.*** *MA-10 cells were pretreated with 50 μM CQ (autophagy inhibitor) (A) and 50 μM U0126 (B) for 1 h, and then co-treated without or with 50 ng/mL FGF9 and 50 μM cordycepin for 24 h, respectively. PrestoBlue assay was then used to assess cell proliferation. MA-10 cells were pretreated with 50 μM*

U0126 or Z-VAD-FMK for 1 h, and then co-treated without or with 50 ng/mL FGF9 and 50 μM cordycepin and for 24 h, respectively. Flow cytometry was used to analyze and determine cell apoptotic status. Percentages of double-positive (late apoptotic), annexin V single-positive (early apoptotic), PI single-positive (necrotic) and double-negative (viable) cells are illustrated, and results in bar graphs are mean ± standard error with at least 3 independent experiments (C). Percentages of double-positive (late apoptotic) plus annexin V single-positive (early apoptotic) cells between treatments were then analyzed by two-way ANOVA with Tukey's multiple comparisons post-tests. Different alphabetical letters above bars represent statistical differences among different treatments; $p < 0.05$.

group had largest size (Fig. 7B). Tumor size in FGF9 plus cordycepin and FGF9 plus cordycepin with U0126 are between cordycepin only group and FGF9 only group (Fig. 7B). Correlated to tumor size, tumor weight in cordycepin only group had lowest weight and mice in FGF9 only group had highest weight (Fig. 7C). Tumor weight in FGF9 plus cordycepin and FGF9 plus cordycepin with U0126 are between cordycepin only group and FGF9 only group (Fig. 7C). The body weights among different groups showed no difference (data not shown).

We further used immunohistochemistry (IHC) assay to examine the expression of cleaved caspase-3 (Fig. 8A), CD31 (Fig. 8B) and p-ERK (Fig. 8C) in

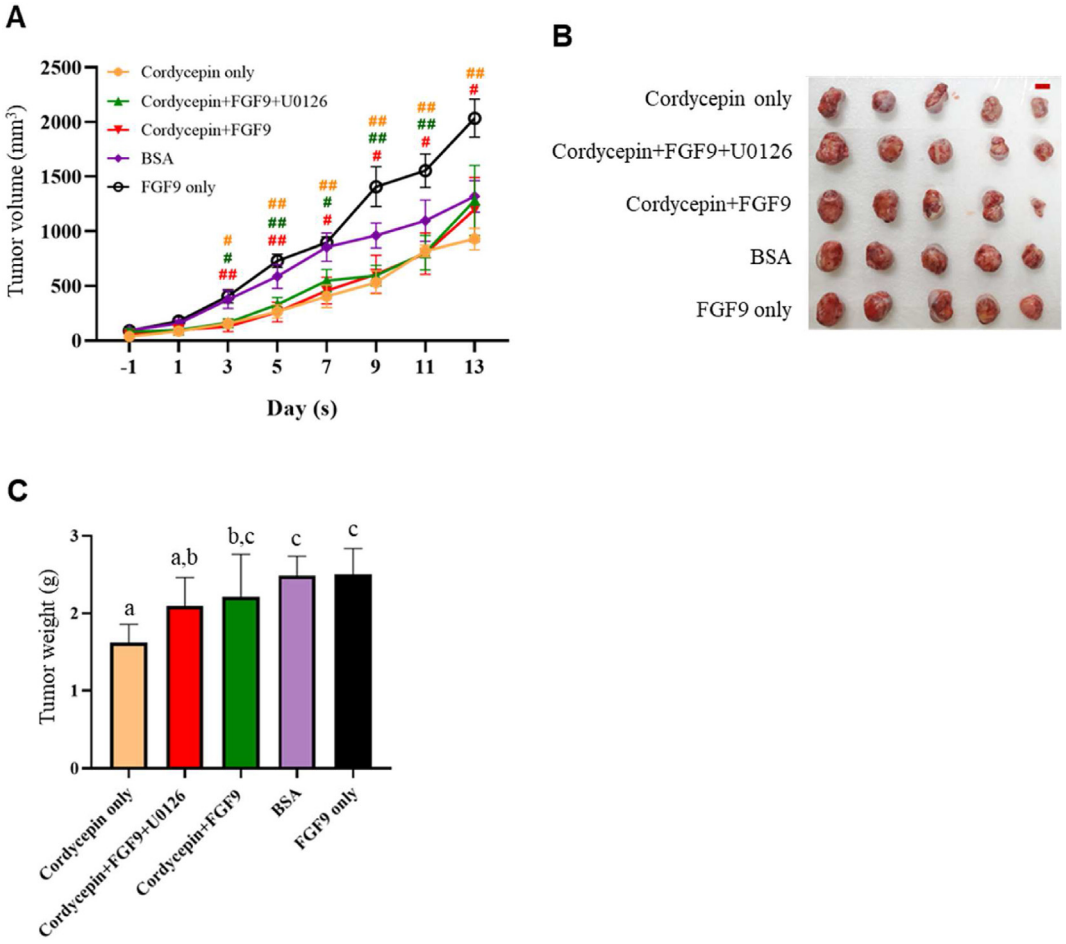

Fig. 7. ***Cordycepin suppressed FGF9-induced MA-10 cell tumorigenesis via ERK pathway in NOD-SCID allograph mouse model.*** *MA-10 cells were subcutaneously injected to the back of NOD-SCID mice. After a palpable tumor formed around 7 days, mice were randomly divided into 5 groups ($n = 5$ in each group); (1) cordycepin (20 mg/kg); (2) FGF9 (5 ng/per mouse) with cordycepin (20 mg/kg) plus U0126 (10.5 mg/kg); (3) FGF9 (5 ng/per mouse) with cordycepin (20 mg/kg); (4) BSA; and (5) FGF9 (5 ng/per mouse) in Day 0, respectively. Mice were sacrificed on the 13th day after drug administration. (A) Illustrates the tumor growth curves among different groups. (B) Illustrates the representative image showing comparative size of tumors among different groups (red scale bar, 10 mm). (C) Illustrates the difference of tumor weights among different groups. Results in (A) tumor growth curves and (C) tumor weights are mean ± standard error from 5 mice among different groups, which were analyzed by two-way ANOVA with Tukey's multiple comparisons post-tests for difference. In (A) tumor growth curves, #$p < 0.05$ and ##$p < 0.01$ in dark yellow color indicate significantly statistical difference between FGF9 only and cordycepin only groups; #$p < 0.05$ and ##$p < 0.01$ in green color indicate significantly statistical difference between FGF9 only and cordycepin + FGF9 + UO126 groups; and #$p < 0.05$ and ##$p < 0.01$ in red color indicate significantly statistical difference between FGF9 only and cordycepin + FGF9 groups, respectively. Different alphabetical letters above histogram in (C) represent statistical differences among different groups; $p < 0.05$.*

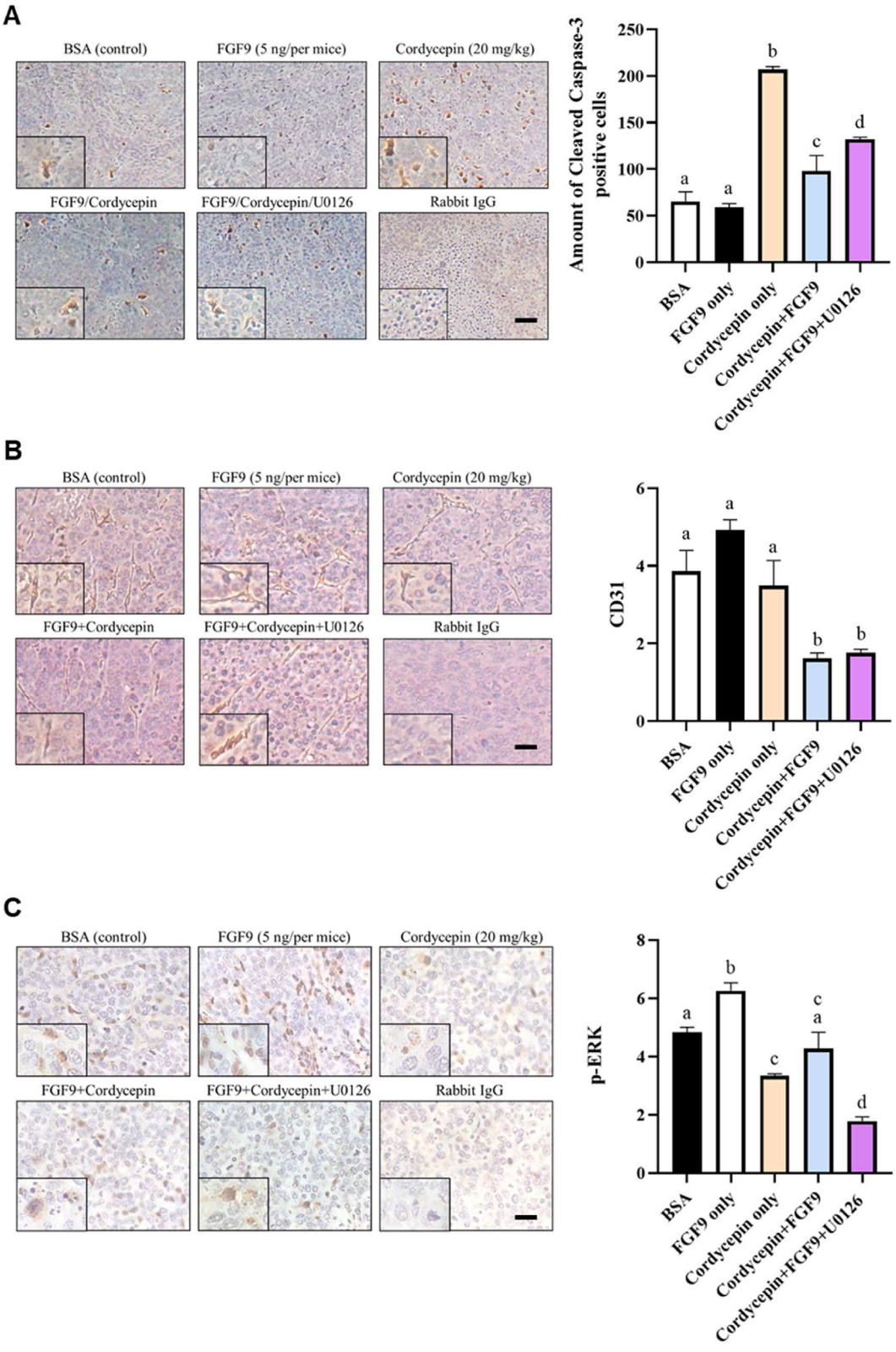

Fig. 8. ***Immunohistochemistry analysis in NOD-SCID mouse model inoculated with MA-10 cells with FGF9 and cordycepin plus U0126 treatments.*** *Tumor samples are from Fig. 7, and the expression patterns of (A) cleaved caspase-3 (brown), (B) CD31 (brown), and (C) p-ERK (brown) in tumor tissue inoculated with MA-10 cells were examined by immunohistochemistry assay (100 × and 200 × in inset; scale bar, 100 μm), which the positive areas were analyzed by ImageJ software. The cell nucleus was stained with hematoxylin. Rabbit IgG was used as a control of the primary antibody. Results in bar graphs are mean ± standard error from 5 mice among different groups, which were analyzed by one-way ANOVA with Tukey's multiple comparisons post-tests for difference. Different alphabetical letters in bar graphs represent statistical differences among different treatments; $p < 0.05$.*

these tumors among different groups. Results show that FGF9 did not induce any cleaved caspase-3 expression, but cordycepin did significantly increase cleaved caspase-3 expression. The expression of cleaved caspase-3 reduced as FGF9 was presented with cordycepin. However, U0126 induced higher expression of cleaved caspase-3 in the treatment of cordycepin plus FGF9 (Fig. 8A).

The expression of CD31 was not significantly different among BSA control, FGF9 only and cordycepin only groups, but FGF9 had tendency to promote blood vessel growth. Indeed, cordycepin did decrease the expression of CD31 under FGF9 treatment. Interestingly, U0126 could not inhibit much more expression of CD31 as compared to cordycepin plus FGF9 groups. These data indicate that cordycepin could reduce blood vessel growth with the presence of FGF9 in mice with MA-10 cell inoculation (Fig. 8B).

The expression of p-ERK significantly increased in FGF9 group, and cordycepin could decrease the expression of p-ERK under FGF9 treatment. Furthermore, U0126 plus could suppress much more expression of p-ERK as compared to cordycepin plus FGF9 group (Fig. 8C).

4. Discussion

Fibroblast growth factors regulate many cell/tissue growth and development processes [43]. In testis, FGFs show different roles involving in development, cell proliferation, differentiation, and apoptosis [1]. However, abnormal expression of FGFs is involved in many cancer developments, such as breast cancer [44], stomach cancer [45], lung cancer [46], prostate cancer [47], and testicular cancer [1,35]. We have shown that FGF9 did induce MA-10 cell proliferation associated with testicular cancer developments *in vitro* and *in vivo* [35]. We have also revealed the anti-cancer effect of cordycepin on FGF9-treated MA-10 cell tumor growth *in vitro* and *in vivo* [36]. In fact, studies have demonstrated that cordycepin has anti-cancer effects in liver cancer [48], colon cancer [49], and breast cancer [50] through the activations of caspase signaling pathways and/or MAPK pathways. However, how did cordycepin inhibit tumor growth in FGF9-induced testicular cancer is still unclear.

In the present study, we reconfirmed that cordycepin did decrease FGF9-treated MA-10 cell viability (Fig. 1). In addition, colony formation assay was applied to ensure that cordycepin could suppress FGF9-treated MA-10 cell survival, and our observation revealed that cordycepin did suppress MA-10 cell proliferation with anti-cancer effects with the presence of FGF9. In fact, study has shown that cordycepin could decrease the count of colony formation in esophageal cancer cells [51]. Thus, our observation is parallel to other findings.

Apoptosis is a process of programmed cell death, accompanied by DNA fragmentation, plasma membrane blebbing and other morphological changes, which usually depends on caspase cascade to make cells death [16]. Previous study shows that cordycepin could induce tumor cell apoptosis through the caspase cascade [48]. In this study, cordycepin could induce the expression of cleaved caspase-3 and PARP proteins in FGF9-induced MA-10 tumor cells. In addition, the expression of cleaved caspase-9, but not caspase-8, could also be stimulated by cordycepin in FGF9-induced MA-10 cells, illustrating intrinsic apoptotic pathway was activated. These observations are not unprecedented with other studies [21–23].

In MA-10 cells, cordycepin didn't induce autophagy, but inhibition of autophagy would enhance cordycepin-induced cell death in FGF9-treated MA-10 cells. These results highly indicate that MA-10 cells might trigger autophagy to protect itself without or with the presence of FGF9. However, longer time and higher dosage cordycepin treatment could possibly overwhelm activate autophagy and then, in turn, induce MA-10 cell apoptosis, ending up with cell death.

In previous study, cordycepin could decrease FGF9-induced MA-10 cell viability through ERK pathway [36]. Studies have shown inhibiting ERK pathway could decrease apoptosis and autophagy [52,53]. However, in other studies, inhibiting ERK pathway could increase apoptosis and autophagy [54,55]. In this study, ERK inhibitor, U0126, was used, and results showed that ERK inhibitor could enhance cell death upon cordycepin in FGF9-treated MA-10 cells, which further confirm cordycepin could inhibit FGF9-induced MA-10 cell growth through the ERK pathway to induce cell death. This observation is consistent with our earlier studies [35,36,41].

Our previous data showed that cordycepin could suppress tumor growth in NOD-SCID mice inoculated with MA-10 cells [35]. In this study, compared with the FGF9 only treatment group, the co-treatment of cordycepin and U0126 also significantly further inhibited tumor size and weight, indicating the combination of cordycepin and U0126 treatment could suppress ERK signaling pathway and then inhibit FGF9-induced tumor growth with MA-10 cell inoculation. In addition, U0126 could enhance the expression of cleaved caspase-3 in MA-10 cell inoculated tumor under cordycepin treatment in

FGF9-treated *in vivo*, suggesting cordycepin did stimulate caspase cascade to suppress MA-10 cell inoculated tumor growth. Therefore, cordycepin combined with ERK inhibitors might be a good potential therapeutic strategy for testicular cancers. A recent study has shown that cordycepin can inhibit pancreatic cancer cell growth *in vitro* and *in vivo* via targeting FGFR2 and blocking ERK signaling, and caspase cascade was stimulated for apoptosis [56]. Accordingly, our data are comparable to other studies.

In conclusion, we demonstrated the anti-cancer effect of cordycepin on FGF9-induced testicular tumor growth *in vitro* and *in vivo*. These data indicate that cordycepin could significantly induce cell death effects in FGF9-treated MA-10 cells through apoptosis, which imply that combination of cordycepin with ERK inhibitor might become a new chemotherapy agent targeting testicular tumor and/or other cancers related to carcinogenic effect of FGF9.

Conflicts of interest and Competing interest statement

Authors declare no conflict of interest and no competing interests.

Acknowledgement

This work was supported by grants from National Science and Technology Council, Taiwan, Republic of China (MOST 110-2320-B-039-079 to LCC and MOST 110-2320-B-006-025 to BMH).

Availability of data

Data used and analyzed of this study are always accessible through authors on reasonable demand.

Authors' contributions

Present study was designed by LCC, YPL and BMH. Experiments were performed by LCC, CYC and YPL. Raw data authenticity was confirmed by LCC and BMH. Data were analyzed by LCC, CYC and YPL. Results were interpreted by LCC, CYC and YPL. Initial manuscript was drafted by LCC, CYC and YPL. Manuscript for important intellectual content was revised by LCC and BMH. Final manuscript was read and approved ensuring accuracy and integrity of the work by all authors.

Ethics approval and consent to participate

Not applicable.

Patient consent for publication

Not applicable.

References

[1] Jiang X, Skibba M, Zhang C, Tan Y, Xin Y, Qu Y. The roles of fibroblast growth factors in the testicular development and tumor. J Diabetes Res 2013;2013:489095.
[2] Itoh N, Nakayama Y, Konishi M. Roles of FGFs as paracrine or endocrine signals in liver development, health, and disease. Front Cell Dev Biol 2016;4:30.
[3] Colvin JS, Green RP, Schmahl J, Capel B, Ornitz DM. Male-to-female sex reversal in mice lacking fibroblast growth factor 9. Cell 2001;104:875–89.
[4] Carré GA, Greenfield A. Characterising novel pathways in testis determination using mouse genetics. Sex Dev 2014;8:199–207.
[5] Abdel-Rahman WM, Kalinina J, Shoman S, Eissa S, Ollikainen M, Elomaa O, et al. Somatic FGF9 mutations in colorectal and endometrial carcinomas associated with membranous beta-catenin. Hum Mutat 2008;29:390–7.
[6] Wang R, Sun Y, Yu W, Yan Y, Qiao M, Jiang R, et al. Downregulation of miRNA-214 in cancer-associated fibroblasts contributes to migration and invasion of gastric cancer cells through targeting FGF9 and inducing EMT. J Exp Clin Cancer Res 2019;38:20.
[7] Donnem T, Al-Shibli K, Al-Saad S, Busund LT, Bremnes RM. Prognostic impact of fibroblast growth factor 2 in non-small cell lung cancer: coexpression with VEGFR-3 and PDGF-B predicts poor survival. J Thorac Oncol 2009;4:578–85.
[8] Nakamura K, Shinozuka K, Yoshikawa N. Anticancer and antimetastatic effects of cordycepin, an active component of Cordyceps sinensis. J Pharmacol Sci 2015;127:53–6.
[9] Yoon SY, Park SJ, Park YJ. The anticancer properties of cordycepin and their underlying mechanisms. Int J Mol Sci 2018;19:3027.
[10] Zhou Y, Guo Z, Meng Q, Lu J, Wang N, Liu H, et al. Cordycepin affects multiple apoptotic pathways to mediate hepatocellular carcinoma cell death. Anticancer Agents Med Chem 2017;17:143–9.
[11] Zhang C, Zhong Q, Zhang XF, Hu DX, He XM, Li QL, et al. Effects of Cordycepin on proliferation, apoptosis and NF-κB signaling pathway in A549 cells. J Chin Med Mater 2015;38:786–9.
[12] Hwang JH, Joo JC, Kim DJ, Jo E, Yoo HS, Lee KB, et al. Cordycepin promotes apoptosis by modulating the ERK-JNK signaling pathway via DUSP5 in renal cancer cells. Am J Cancer Res 2016;6:1758–71.
[13] Guo YJ, Pan WW, Liu SB, Shen ZF, Xu Y, Hu LL. ERK/MAPK signalling pathway and tumorigenesis. Exp Ther Med 2020;19:1997–2007.
[14] Santarpia L, Lippman SM, El-Naggar AK. Targeting the MAPK-RAS-RAF signaling pathway in cancer therapy. Expert Opin Ther Targets 2012;16:103–19.
[15] Katoh M, Nakagama H. FGF receptors: cancer biology and therapeutics. Med Res Rev 2014;34:280–300.
[16] Elmore S. Apoptosis: a review of programmed cell death. Toxicol Pathol 2007;35:495–516.
[17] Wyllie AH. Apoptosis: an overview. Br Med Bull 1997;53:451–65.
[18] You Y, Cheng AC, Wang MS, Jia RY, Sun KF, Yang Q, et al. The suppression of apoptosis by α-herpesvirus. Cell Death Dis 2017;8:e2749.
[19] Ashkenazi A, Dixit VM. Death receptors: signaling and modulation. Science 1998;281:1305–8.
[20] Carneiro BA, El-Deiry WS. Targeting apoptosis in cancer therapy. Nat Rev Clin Oncol 2020;17:395–417.
[21] Oltvai ZN, Milliman CL, Korsmeyer SJ. Bcl-2 heterodimerizes in vivo with a conserved homolog, Bax, that accelerates programmed cell death. Cell 1993;74:609–19.

[22] Brentnall M, Rodriguez-Menocal L, De Guevara RL, Cepero E, Boise LH. Caspase-9, caspase-3 and caspase-7 have distinct roles during intrinsic apoptosis. BMC Cell Biol 2013;14:32.
[23] Mishra AP, Salehi B, Sharifi-Rad M, Pezzani R, Kobarfard F, Sharifi-Rad J, et al. Programmed cell death, from a cancer perspective: an overview. Mol Diagn Ther 2018;22:281–95.
[24] McIlwain DR, Berger T, Mak TW. Caspase functions in cell death and disease. Cold Spring Harbor Perspect Biol 2013;5: a008656.
[25] Cicchini M, Karantza V, Xia B. Molecular pathways: autophagy in cancer–a matter of timing and context. Clin Cancer Res 2015;21:498–504.
[26] Mizushima N, Komatsu M. Autophagy: renovation of cells and tissues. Cell 2011;147:728–41.
[27] Levine B, Yuan J. Autophagy in cell death: an innocent convict? J Clin Invest 2005;115:2679–88.
[28] Nakatogawa H, Suzuki K, Kamada Y, Ohsumi Y. Dynamics and diversity in autophagy mechanisms: lessons from yeast. Nat Rev Mol Cell Biol 2009;10:458–67.
[29] Chen Y, Klionsky DJ. The regulation of autophagy - unanswered questions. J Cell Sci 2011;124:161–70.
[30] Eisenberg-Lerner A, Bialik S, Simon HU, Kimchi A. Life and death partners: apoptosis, autophagy and the cross-talk between them. Cell Death Differ 2009;16:966–75.
[31] Yao F, Zhang M, Chen L. 5'-Monophosphate-activated protein kinase (AMPK) improves autophagic activity in diabetes and diabetic complications. Acta Pharm Sin B 2016;6:20–5.
[32] Arakawa S, Honda S, Yamaguchi H, Shimizu S. Molecular mechanisms and physiological roles of Atg5/Atg7-independent alternative autophagy. Proc Jpn Acad Ser B Phys Biol Sci 2017;93:378–85.
[33] Novak I, Kirkin V, McEwan DG, Zhang J, Wild P, Rozenknop A, et al. Nix is a selective autophagy receptor for mitochondrial clearance. EMBO Rep 2010;11:45–51.
[34] Kumar S, Park HS, Lee K. Jagged1 intracellular domain modulates steroidogenesis in testicular Leydig cells. PLoS One 2020;15:e0244553.
[35] Chang MM, Lai MS, Hong SY, Pan BS, Huang H, Yang SH, et al. FGF9/FGFR2 increase cell proliferation by activating ERK1/2, Rb/E2F1, and cell cycle pathways in mouse Leydig tumor cells. Cancer Sci 2018;109:3503–18.
[36] Chang MM, Hong SY, Yang SH, Wu CC, Wang CY, Huang BM. Anti-cancer effect of cordycepin on FGF9-induced testicular tumorigenesis. Int J Mol Sci 2020;21(21): 8336.
[37] Franken NA, Rodermond HM, Stap J, Haveman J, van Bree C. Clonogenic assay of cells in vitro. Nat Protoc 2006;1: 2315–9.
[38] Juan WS, Mu YF, Wang CY, So EC, Lee YP, Lin SC, et al. Arsenic compounds activate MAPK and inhibit Akt pathways to induce apoptosis in MA-10 mouse Leydig tumor cells. Cancer Med 2023;12:3260–75.
[39] Tomayko MM, Reynolds CP. Determination of subcutaneous tumor size in athymic (nude) mice. Cancer Chemother Pharmacol 1989;24:148–54.
[40] Fan TJ, Han LH, Cong RS, Liang J. Caspase family proteases and apoptosis. Acta Biochim Biophys Sin 2005;37:719–27.
[41] Pan BS, Wang YK, Lai MS, Mu YF, Huang BM. Cordycepin induced MA-10 mouse Leydig tumor cell apoptosis by regulating p38 MAPKs and PI3K/AKT signaling pathways. Sci Rep 2015;5:13372.
[42] Mushtaque M, Shahjahan M. Reemergence of chloroquine (CQ) analogs as multi-targeting antimalarial agents: a review. Eur J Med Chem 2015;90:280–95.
[43] Xie Y, Su N, Yang J, Tan Q, Huang S, Jin M, et al. FGF/FGFR signaling in health and disease. Signal Transduct Target Ther 2020;5:181.
[44] Yu Z, Lou L, Zhao Y. Fibroblast growth factor 18 promotes the growth, migration and invasion of MDA-MB-231 cells. Oncol Rep 2018;40:704–14.
[45] Zhang J, Tang PMK, Zhou Y, Cheng ASL, Yu J, Kang W, et al. Targeting the oncogenic FGF-FGFR axis in gastric carcinogenesis. Cells 2019;8:637.
[46] Wang K, Ji W, Yu Y, Li Z, Niu X, Xia W, et al. FGFR1-ERK1/2-SOX2 axis promotes cell proliferation, epithelial-mesenchymal transition, and metastasis in FGFR1-amplified lung cancer. Oncogene 2018;37:5340–54.
[47] Kwabi-Addo B, Ozen M, Ittmann M. The role of fibroblast growth factors and their receptors in prostate cancer. Endocr Relat Cancer 2004;11:709–24.
[48] Shao LW, Huang LH, Yan S, Jin JD, Ren SY. Cordycepin induces apoptosis in human liver cancer HepG2 cells through extrinsic and intrinsic signaling pathways. Oncol Lett 2016;12:995–1000.
[49] Lee SJ, Moon GS, Jung KH, Kim WJ, Moon SK. c-Jun N-terminal kinase 1 is required for cordycepin-mediated induction of G2/M cell-cycle arrest via p21WAF1 expression in human colon cancer cells. Food Chem Toxicol 2010;48: 277–83.
[50] Liu C, Qi M, Li L, Yuan Y, Wu X, Fu J. Natural cordycepin induces apoptosis and suppresses metastasis in breast cancer cells by inhibiting the Hedgehog pathway. Food Funct 2020;11:2107–16.
[51] Xu JC, Zhou XP, Wang XA, Xu MD, Chen T, Chen TY, et al. Cordycepin induces apoptosis and G2/M phase arrest through the ERK pathways in esophageal cancer cells. J Cancer 2019;10:2415–24.
[52] Cagnol S, Chambard JC. ERK and cell death: mechanisms of ERK-induced cell death–apoptosis, autophagy and senescence. FEBS J 2010;277:2–21.
[53] Wang A, Zhang H, Liang Z, Xu K, Qiu W, Tian Y, et al. U0126 attenuates ischemia/reperfusion-induced apoptosis and autophagy in myocardium through MEK/ERK/EGR-1 pathway. Eur J Pharmacol 2016;788:280–5.
[54] Ye H, Zhang Y, Wang Y, Xia J, Mao X, Yu X. The restraining effect of baicalein and U0126 on human cervical cancer cell line HeLa. Mol Med Rep 2017;16:957–63.
[55] Bryant KL, Stalnecker CA, Zeitouni D, Klomp JE, Peng S, Tikunov AP, et al. Combination of ERK and autophagy inhibition as a treatment approach for pancreatic cancer. Nat Med 2019;25:628–40.
[56] Li XY, Tao H, Jin C, Du ZY, Liao WF, Tang QJ, et al. Cordycepin inhibits pancreatic cancer cell growth in vitro and in vivo via targeting FGFR2 and blocking ERK signaling. Chin J Nat Med 2020;18:345–55.